

Communication

Circular Dichroism Reflectance Anisotropy of Chiral Atomically Thin Films

Ilaria Tomei ¹, Filippo Pierucci ¹, Beatrice Bonanni ¹ , Anna Sgarlata ¹ , Massimo Fanfoni ¹, Seong-Jun Yang ^{2,3}, Cheol-Joo Kim ^{2,3} and Claudio Goletti ^{1,*} 

¹ Department of Physics, Università di Roma Tor Vergata, Via della Ricerca Scientifica 1, 00133 Rome, Italy; iilaria.tomei@gmail.com (I.T.); pieruccifilippo97@gmail.com (F.P.); bonanni@roma2.infn.it (B.B.); sgarlata@roma2.infn.it (A.S.); fanfoni@roma2.infn.it (M.F.)

² Center for van der Waals Quantum Solids, Institute for Basic Science (IBS), Pohang 37673, Republic of Korea; ysjsj954@ibs.re.kr (S.-J.Y.); kimcj@postech.ac.kr (C.-J.K.)

³ Department of Chemical Engineering, Pohang University of Science and Technology (POSTECH), Pohang 37673, Republic of Korea

* Correspondence: goletti@roma2.infn.it

Abstract: Recently, a technical modification of a Reflectance Anisotropy Spectroscopy (RAS) spectrometer has been proposed to investigate the circular dichroism (CD) of samples instead of the normally studied linear dichroism. CD-RAS measures the anisotropy of the optical properties of a sample under right-handed and left-handed circularly polarized light. Here, we present the application of CD-RAS to measure the circular dichroism of a twisted bilayer of graphene, purposely prepared as a possible substrate for the adsorption of thin molecular layers, in air, in liquid or in a vacuum. This result demonstrates the performance of the apparatus and shows interesting perspectives for the investigation of chiral organic assemblies deposited in solid film.

Keywords: reflectance anisotropy spectroscopy; circular dichroism; chiral layers; twisted graphene bilayers



Citation: Tomei, I.; Pierucci, F.; Bonanni, B.; Sgarlata, A.; Fanfoni, M.; Yang, S.-J.; Kim, C.-J.; Goletti, C. Circular Dichroism Reflectance Anisotropy of Chiral Atomically Thin Films. *Chemosensors* **2024**, *12*, 170. <https://doi.org/10.3390/chemosensors12090170>

Received: 22 July 2024

Revised: 11 August 2024

Accepted: 20 August 2024

Published: 24 August 2024



Copyright: © 2024 by the authors. Licensee MDPI, Basel, Switzerland. This article is an open access article distributed under the terms and conditions of the Creative Commons Attribution (CC BY) license (<https://creativecommons.org/licenses/by/4.0/>).

1. Introduction

When Lord Kelvin, in 1893, in a Robert Boyle Lecture at Oxford University introduced for the first time the term chirality, saying that “any geometrical figure, or group of points, is chiral, if its image in a plane mirror, ideally realized, cannot be brought to coincide with itself” [1], he was very likely not aware of having coined a word whose fascinating sound would span in forthcoming years from physics to chemistry, from medicine to mathematics, and has pervaded modern science from the physics of elementary particles to astronomy, from the chemistry of the origin of life to the nanotechnology, from the preparation of drugs to chemical sensors [2–6].

In the development of chiral materials, the flexibility of carbon atoms’ chemistry has been often exploited in building the backbone of new molecular elements, while versatile and tunable molecular systems (such as porphyrins, an unsurpassed building block [7,8]) have been manipulated and then assembled in more complex structures, where chirality can appear also at the supramolecular level [9,10].

If organic chemistry reveals an inexhaustible forge of new molecules for surprising applications, in the case of sensors two issues arise: (i) the necessity to move to solid-state organic layers but maintaining chirality; (ii) the investigation of the selective interactions between analyte and sensor useful to enantiomeric recognition [11].

Here, new challenges arise: effective deposition methods [12,13], the use of non-transparent substrates, easy-to-use experimental techniques and exhibiting the necessary sensitivity to chirality [14,15]. A long tradition of chemistry laboratories (and not only) would point in the direction of optical techniques: experiments by spectropolarimeters

that measure circular dichroism (CD), i.e., the differential absorption of left- and right-handed polarized light, represent a common practice (or better a necessary step) in a characterization protocol of samples. However, commercial CD spectrometers do not allow high flexibility in the design of the optical path and offer limited room for the investigated sample: it is definitely not easy pairing these apparatuses with Ultra High Vacuum (UHV) systems (in case of depositions from evaporation cells, for example), with electrochemical cells or more generally with other complex experimental configurations.

Recently, we proposed to use a Reflectance Anisotropy Spectroscopy (RAS) apparatus with a new “open” and pliant configuration for measuring CD (hereafter indicated as circular dichroism RAS, CD-RAS) [16].

RAS is an optical technique exhibiting high sensitivity to very low thickness of matter (in the order of a few Angstroms, and even below), thus giving the possibility to study the structure and the electronic properties of surfaces, interfaces and very thin layers deposited onto solid substrates [17]. It can be used in a vacuum or in a UHV [18–21], but also in atmosphere (as it does not suffer any limitation due to pressure, contrary to spectroscopies using electrons or charged particles as probes), or in transparent media to investigate surfaces/layers and interfaces immersed in liquids [22–24]. RAS has been also applied to study organic samples, for example layers grown by Organic Molecular Beam Epitaxy (OMBE) [25] or deposited in a UHV [26].

Until now, all the published RAS results concern the anisotropy of the reflectance by linearly polarized light. Recently, we have extended the application of the same technique to measure in transmittance the CD by a proper modification of the experimental apparatus, opening intriguing perspectives in the investigation of chirality [16].

It is simple to show that a CD signal measured in reflectance mode from a chiral layer is null, whatever its thickness is. This obliges experimentalists to choose the transmission mode for measurements of chiral solutions and layers, thus obviously limiting the solid substrate to its transparency region. As an additional limit, such a substrate (in the vis–UV range, usually glass or quartz, flat and inert, is used) offers almost no opportunity to modulate or construct the chiral structure of the deposited layer, while substrate engineering could play an active role inducing chirality in an individual nanostructure by a proper choice of its structure, or driving it by designed molecule–substrate interactions [27,28].

The use of ultrathin, a few monolayers thick, layers of graphene deposited onto UV quartz could allow both these constraints to be overcome [29]. In fact, while the extremely reduced thickness of the graphene layer makes it virtually transparent, the possibility of growing bilayers of graphene according to a projected twist angle offers the opportunity to control the possible chiral signal [12,28]. Finally, the peculiar hexagonal symmetry of graphene cancels out the possible contribution coming from linear dichroism of graphite samples, excluding artifacts that in some cases could modify or even hide the dichroism results [30–32].

In this paper, we present the CD-RAS spectra of two purposely prepared twisted graphene bilayers, arranged in two enantiomeric forms, that push the sensitivity of our apparatus towards a low level of the ellipticity signal. This preliminary result represents an interesting starting point to deposit thin and ultrathin molecular chiral or achiral layers on these graphene substrates.

2. Materials and Methods

2.1. The CD-RAS Apparatus

A RAS spectrometer is basically an ellipsometer at near-normal incidence; this simple variation in the experimental apparatus with respect to a traditional ellipsometry set-up (where the incidence angle can be varied) strongly simplifies the interpretation of the data. The detection of a non-null optical anisotropy is sometimes a significant result per se, representing the properties of the sample in terms of the existence of some kind of order at the microscopic level. Nevertheless, a deeper comprehension of the investigated system still

requires a further analysis of the optical anisotropy experimental data by a mathematical deconvolution of the dielectric functions, through modelling of the system [17].

The definition of RAS signal is reported in Formula (1). It expresses $\Delta R/R$ as the ratio between the difference ΔR in the light intensity R_α and R_β reflected by the sample for a beam polarized in two different and perpendicular polarization states α and β , and their average $R = (R_\alpha + R_\beta)/2$, as a function of photon energy [17,33]:

$$\Delta R/R = 2 (R_\alpha - R_\beta)/(R_\alpha + R_\beta) \quad (1)$$

If linearly polarized light is used in the experiments, the electric field of light is alternatively directed along two directions α and β , mutually orthogonal and aligned with the main anisotropy axes of the sample surface plane. This is the common application of RAS in the scientific community [17]. In CD-RAS, on the contrary, the light shone onto the sample is modulated between right-handed and left-handed circularly polarized light, with the resulting signal carrying information about the CD of the investigated system [16].

The modulation of the light polarization in both cases is due to the phase shift introduced by the piezo-elastic modulator (PEM, driven by an oscillating circuit at the resonance frequency ν_0 of the piezoelectric crystal) [16,34] between the two light beams propagating along the ordinary and extraordinary axis of the PEM itself. The PEM distinguishes the two cases reported above as follows: (i) when the phase shift equals $\pm\pi$, the linear polarization of light after the PEM is modulated at exactly $2\nu_0$ between two orthogonal, independent states x and y ; (ii) if the PEM introduces a phase shift equal to $\pm\pi/2$, the outgoing light is alternatively modulated at frequency ν_0 between right-handed and left-handed circularly polarized light. This second case holds in CD-RAS.

The time-dependence of the light polarization states for circularly polarized light after the passage through the PEM for a phase shift equal to $\pm\pi/2$ is shown in the right panel of Figure 1. The polarization oscillates between circularly left-handed and circularly right-handed polarization states, at the same frequency ν_0 of the PEM. In addition, a relic linear polarization contribution is still present in the signal (just for one of two orthogonal independent states, in the figure labelled “ α ”), the latter at a frequency that is twice the PEM frequency. Consequently, if a lock-in amplifier is tuned at a frequency equal to ν_0 , the only contribution in the signal output after the detector will be due to the circularly polarized light modulation.

The CD-RAS apparatus is described in ref. [16]. In the left panel of Figure 1, the version used in experiments reported in this article has been drawn: it is the Safarov/Berkovits spectrometer (see refs. [16,33,35]), with one polarizer. The light beam from a Xe lamp (75 W, Hamamatsu Photonics, Sunayamacho, Japan) passes through a Glan Taylor polarizer (Melles Griot, Carlsbad, CA, USA) whose axis is carefully oriented at 45° , to linearly polarize the light before it enters a home-made piezo-elastic modulator (transparent optical head in quartz, glued with beeswax to a piezo-elastic quartz crystal). After the beam is transmitted through the sample, it is reflected on an oxidized Si(100) surface, which—being isotropic for linearly polarized light—does not introduce artifacts in the signal. Finally, the beam enters a grating monochromator (HR-10, Jobin Yvon, Paris, France) and is collected on a photomultiplier (Hamamatsu Photonics, Japan)). The control of the whole apparatus is performed through a unit engineered in Ioffe Institute (St. Petersburg, Russia Russian Federation). All the lenses are biconvex, in CaF_2 .

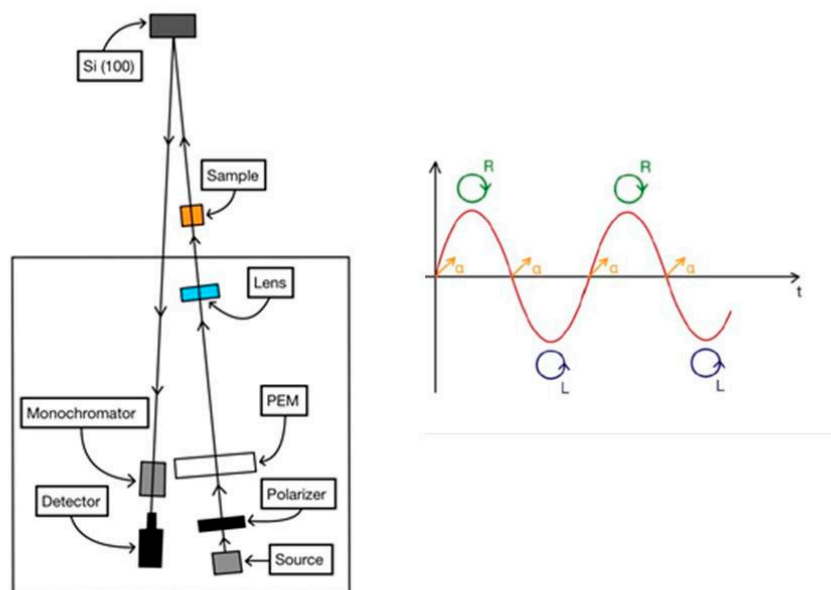


Figure 1. (Left panel): Sketch of the CD-RAS experimental apparatus. The version here reported is the Safarov /Berkovits spectrometer (see refs. [16,33,35]), with one polarizer. After passing the sample, the light beam is reflected back by an isotropic Si(100) sample and collected on the detector through the monochromator. (Right panel): Sketch of the polarization of the light beam after the PEM, for an applied voltage value such that the phase shift is $\Delta\varphi = \pi/2$. The red curve represents (vs. time) the voltage driving the PEM at the frequency ν_0 . At $V = 0$ volts, the polarization is linear, here indicated as α (yellow arrows). When the voltage reaches its maximum, the resulting polarization is circular and right-handed (green circles). When the voltage reaches its minimum, the resulting polarization is circular and left-handed (blue circles). The oscillation frequency of the signal between the two states of circular polarization is evidently ν_0 . The frequency of the linearly polarized signal is $2\nu_0$.

The experiments are necessarily performed in transmission, making the term “reflectance” in the acronym CD-RAS somewhat inappropriate. The CD-RAS signal is then more properly defined as follows:

$$\Delta I/I = 2(I_\alpha - I_\beta)/(I_\alpha + I_\beta) \quad (2)$$

In this case, I_α and I_β are the transmitted light intensities measured after light has passed through the sample, while the beam is alternatively polarized in two different and independent circular polarization states α and β .

When CD-RAS data are compared with the ones obtained by a commercial spectrometer, we have to consider that we measure the intensity modulation $\Delta I/I$ of the signal (see Formula (2)), while by using a commercial spectrometer [36], one measures the ellipticity of the beam of light after it is transmitted through the sample. This is the result of the composition (generally associated to the elliptic polarization of light) of the two circularly polarized states, which have the same intensity when they “touch” the sample, but then are absorbed in a different way.

CD spectra are commonly reported in terms of the ellipticity θ and measured in mdeg units. In ref. [16], the proportionality between the ellipticity θ and the $\Delta I/I$ result of a CD-RAS experiment has been demonstrated:

$$\Delta I/I \propto \theta \quad (3)$$

2.2. The Substrate

Chiral twisted bilayers of graphene were prepared by layer-by-layer stacking of unidirectionally grown graphene films on germanium substrates [37]. The interlayer rotational angle (θ) and polarity were controlled during the stacking. Stackings with rotation of the

top graphene towards anticlockwise and clockwise correspond to left- and right-handed films, as depicted in Figure 2. About the terminology throughout the manuscript, the wording “right-handed/left-handed twisted bilayer graphene” means “right-handed/left-handed enantiomer”. The films were transferred onto an ultrathin quartz substrate. In these chiral twisted bilayer graphene films, the angle θ and handedness are controlled uniformly over several millimetres millimeters with a high yield of interlayer coupling. For more details, the reader is invited to examine the Methods and Supplementary of [37].

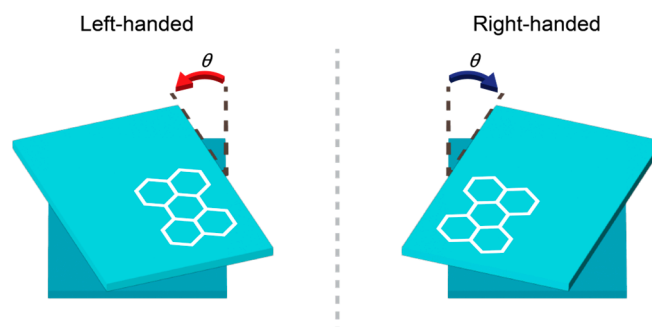


Figure 2. Schematic of left- and right-handed twisted bilayer graphene films connected by a mirror plane (vertical line). The rotation angle θ and polarity determine the spectral energy and the sign of the chiro-optical property, respectively.

The careful and delicate preparation of these twisted bilayer graphene films represents a significant example of the possibility to assemble two-dimensional (2D) materials into artificial structures, exploiting the degrees of freedom offered by Van der Waals structures to exceed the limits existing in traditional growth methods for the fabrication of advanced nanodevices. In fact, growth and assembly here represent two independent steps in the whole process, thus combining materials whose growth conditions would be otherwise incompatible. Furthermore, as adjacent layers are not chemically bonded, the weak Van der Waals interactions enable a very high control of the orientation of individual crystalline layers, thus producing a high possibility to manipulate the atomic configurations in the resulting structure and in principle paving the way to a huge number of possible combinations [37].

The optical circular dichroism of graphene films was measured using a Jasco circular dichroism spectrometer (J-815) (Jasco, Tokyo, Japan), in transmission mode with the light beam perpendicular to the film planes over a circular area of 2 mm in diameter. Lock-in measurements were conducted by alternating at 50 kHz between left-handed and right-handed circularly polarized lights.

3. Results

Ellipticity spectra, or circular dichroism (CD) spectra, measured from the chiral twisted bilayer graphene films with $\theta = 25.8^\circ$ (red: left-handed) and $\theta = 23.1^\circ$ (blue: right-handed) are shown in Figure 3. The CD spectra of left- and right-handed twisted bilayer graphene show two evident peaks, denoted Peak A and B, with an amplitude in the order of 1 mdeg, like a previous report [38]. The large peak energy and the sign amplitude observed in twisted bilayer graphene films can be tuned using θ and the rotational polarity of the stacked layer [37,38]. Also, the CD spectrum of a single-layer graphene is reported for comparison, to realize its negligible value over the complete photon energy range.

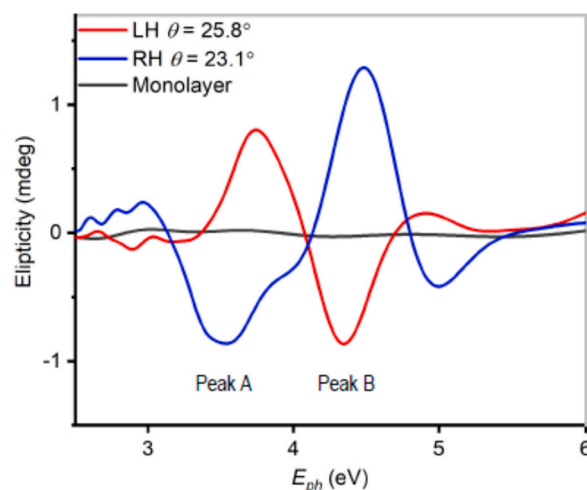


Figure 3. Ellipticity spectra of the chiral twisted bilayer graphene films with $\theta = 25.8^\circ$ (red: left-handed) and $\theta = 23.1^\circ$ (blue: right-handed). Two peaks (here labelled as A and B) are clear in the spectra of two enantiomers.

When CD is measured, great care is necessary to depurate the signal from artifacts coming from the linear dichroism and the linear birefringence of the sample, usually orders of magnitude higher. This has been explicitly discussed in several interesting papers [30–32], which suggest methods useful to isolate the true effect of chiral materials coming from the intrinsic electronic properties or from the supramolecular structure. In fact, experimental CD spectra contain parasitic artifacts, originating from (i) the linear birefringence and the linear dichroism of the sample and (ii) the non-ideal characteristics of optical instruments.

In our case, given the very small value of the graphene bilayer CD (in the order of a millideg and even less), some caution must be taken. We then first measured the RAS anisotropy (i.e., the linear dichroism) of the two bilayers, which is expected to be null due to the hexagonal symmetry of the unit cell. This is plainly shown in the $\Delta R/R$ spectrum reported in Figure 4, which establishes the necessary (but not sufficient) condition to measure CD, otherwise impossible in the presence of linear effects [30–32]. Also, the birefringence effect is expected to be zero, as for our experimental CD-RAS set-up, we have chosen the Safarov–Berkovits configuration (that is without the analyser, see ref. [28]) [39]. In conclusion, the output from the CD-RAS system is *almost* the *true* ellipticity of the two enantiomers.

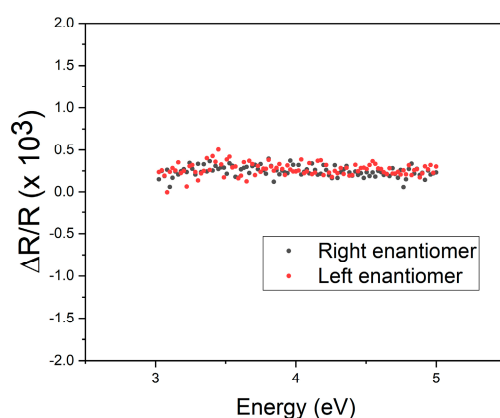


Figure 4. $\Delta R/R$ spectra of the two graphene bilayers, deposited onto quartz. The two enantiomers (right-handed: black circles; left-handed: red circles) are reported. The RAS data have been taken by using linearly polarized light and an Aspnes-like apparatus (with two polarizers, see ref. [17,33]). The residual structureless background in this case has not been subtracted. The flat, almost-zero line measured in both cases reflects the isotropy of the hexagonal graphene unit cell.

CD-RAS spectra have been measured in transmission mode in the range of 3–4 eV and are reported in Figure 5. Despite noise (notice its amplitude, in the order of the signal error bar, 1×10^{-4}), the two enantiomers are clearly resolved. The spectra have been limited to the ellipticity peak at lower photon energies (A in Figure 3), due to the spectral sensitivity of our apparatus that in the UVB range is more than a factor of 10 lower than in the UVA range. The spectra (of the left-handed and right-handed enantiomers) correctly exhibit opposite signs, while (given the scattering of the data) it is not straightforward to conclude if the signal maxima are or are not coincident (compare Peak A in Figure 3). According to a simple polynomial fit (see the two full lines), one could obtain about 3.6 eV for the maximum of the left-handed enantiomer and about 3.5 eV for the right-handed enantiomer. The reduced amplitude (about one-quarter of that measured by the commercial CD spectrometer, see Figure 3) is probably due to the partial oxidation of the graphene, hampering the effect [40]. Although the substrate has been stored under vacuum after the preparation and then after each measurement stage, the experiments (in air) were prolonged for some weeks to obtain the result, thus deteriorating the original signal.

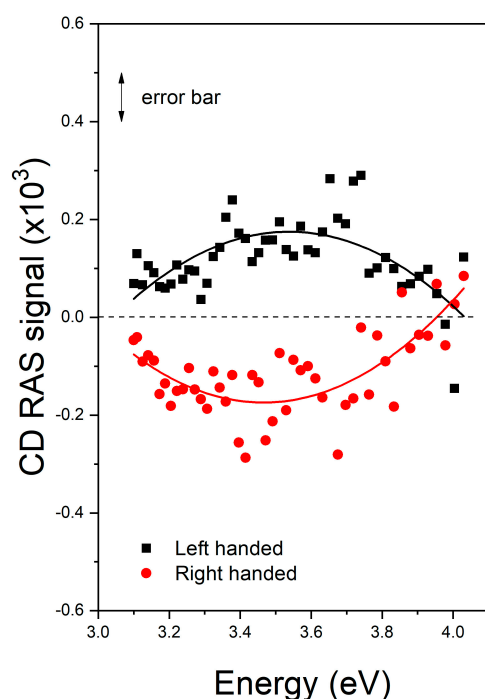


Figure 5. CD-RAS of two enantiomers of the twisted graphene bilayer (described in Section 2.2, whose characterization has been reported in Section 3), measured by a CD-RAS spectrometer with only one polarizer (that is, without analyser, see ref. [33]). Upper curve: left-handed enantiomer (black squares); lower curve: right-handed enantiomer (red circles). The background spectrum due to the optics has been subtracted in both cases. The experimental error bar (equivalent to 1×10^{-4}) is reported. The curves show two maxima with opposite sign. Given the scattering of the data, it is not straightforward to conclude if the signal maxima are or are not coincident. According to a simple polynomial fit (see the two full lines), one could obtain about 3.6 eV for maximum of the left-handed enantiomer and about 3.5 eV for the right-handed enantiomer.

4. Conclusions

We have presented the ellipticity spectra of two enantiomers of twisted graphene bilayers, intentionally prepared. The results presented confirm the good sensitivity of our CD-RAS apparatus and open the way to further developments, where the twisted bilayers will be used as substrates for the deposition of selected chiral molecules in experiments conducted on organic and biological ultrathin layers to investigate the fascinating issue of the origin of life on the early Earth [41–44].

Van der Waals 2D homobilayers offer exciting opportunities: through the control of the twist angle between overlying layers of two-dimensional materials, their electrical properties can be tuned and manipulated, leading to a fascinating physics where the control of chirality could produce innovative optoelectronic devices [45–47]. Recently, it has been reported that chirality from the twist interface of graphene can be transferred to achiral few-layer graphene, producing a strong chiroptical response [48]. In that case, Raman spectroscopy with circularly polarized light has been used. We believe that CD-RAS could also offer intriguing possibilities of application in the future.

Author Contributions: Conceptualization, C.G., C.-J.K. and S.-J.Y.; methodology, C.G. and I.T.; validation, C.G.; formal analysis, F.P., A.S., M.F. and B.B.; CD-RAS experiments, C.G., I.T. and F.P.; preparation of graphene bilayers, S.-J.Y.; writing—original draft preparation, C.G. and C.-J.K.; writing—review and editing, B.B., A.S. and M.F.; supervision, C.G.; funding acquisition, C.G. All authors have read and agreed to the published version of the manuscript.

Funding: Part of the research activities described in this paper were carried out with contribution of the Next Generation EU funds within the National Recovery and Resilience Plan (PNRR), Mission 4—Education and Research, Component 2—From Research to Business (M4C2), Investment Line 3.1—Strengthening and creation of Research Infrastructures, Project IR0000034—“STILES—Strengthening the Italian Leadership in ELT and SKA”. S.-J.Y. and C.-J.K. acknowledge support from the National R&D Program through the National Research Foundation of Korea, funded by the Ministry of Science and ICT (2022M3H4A1A01012718).

Data Availability Statement: The data presented in this study are available on request from the corresponding author.

Acknowledgments: We acknowledge useful discussions about chiral organic systems with Roberto Paolesse (Chemistry Department, University of Rome Tor Vergata).

Conflicts of Interest: The authors declare no conflicts of interest.

References

1. Kelvin, L. *The Molecular Tactics of a Crystal*; Clarendon Press: Oxford, UK, 1894.
2. Barron, L.D. Symmetry and molecular chirality. *Chem. Soc. Rev.* **1986**, *15*, 189. [[CrossRef](#)]
3. Yan, B. Structural Chirality and Electronic Chirality in Quantum Materials. *Annu. Rev. Mater. Res.* **2024**, *54*, 97–115. [[CrossRef](#)]
4. Barron, L.D. Symmetry and chirality: Where physics shakes hands with chemistry and biology. *Isr. J. Chem.* **2021**, *61*, 517. [[CrossRef](#)]
5. Zor, E.; Bingol, H.; Ersoz, M. Chiral sensors. *TrAC Trends Anal. Chem.* **2019**, *121*, 115662. [[CrossRef](#)]
6. Brandenburg, A. Chirality in Astrophysics. In *Chiral Matter—Proceedings of the Nobel Symposium*; World Scientific Publishing Co. Pte. Ltd.: Singapore, 2023; Volume 167, p. 15.
7. Zhang, L.; Wang, T.; Jiang, J.; Liu, M. Chiral porphyrin assemblies. *Aggregate* **2023**, *4*, e198. [[CrossRef](#)]
8. Kingsbury, C.J.; Senge, M.O. The shape of porphyrins. *Coord. Chem. Rev.* **2021**, *431*, 213760. [[CrossRef](#)]
9. Liu, M.; Zhang, L.; Wang, T. Supramolecular chirality in self-assembled systems. *Chem. Rev.* **2015**, *115*, 7304. [[CrossRef](#)]
10. Monti, D. Recent Advancements in Chiral Porphyrin Self-Assembly. In *Synthesis and Modification of Porphyrinoids—Topics in Heterocyclic Chemistry*; Paolesse, R., Ed.; Springer: Berlin/Heidelberg, Germany, 2014; Volume 33, p. 231.
11. Hembury, G.A.; Borovkov, V.V.; Inoue, Y. Chirality-sensing supramolecular systems. *Chem. Rev.* **2008**, *108*, 1–73. [[CrossRef](#)]
12. Hwang, M.; Yeom, B. Fabrication of chiral materials in nano-and microscale. *Chem. Mater.* **2021**, *33*, 807. [[CrossRef](#)]
13. Han, Z.; Wang, F.; Sun, J.; Wang, X.; Tang, Z. Recent advances in ultrathin chiral metasurfaces by twisted stacking. *Adv. Mater.* **2023**, *35*, 2206141. [[CrossRef](#)] [[PubMed](#)]
14. Mu, X.; Hu, L.; Cheng, Y.; Fang, Y.; Sun, M. Chiral surface plasmon-enhanced chiral spectroscopy: Principles and applications. *Nanoscale* **2021**, *13*, 581. [[CrossRef](#)]
15. Huang, S.; Xu, X. Optical chirality detection using a topological insulator transistor. *Adv. Opt. Mater.* **2021**, *9*, 2002210. [[CrossRef](#)]
16. Tomei, I.; Bonanni, B.; Sgarlata, A.; Fanfoni, M.; Martini, R.; Di Filippo, I.; Magna, G.; Stefanelli, M.; Monti, D.; Paolesse, R.; et al. Chiral Porphyrin Assemblies Investigated by a Modified Reflectance Anisotropy Spectroscopy Spectrometer. *Molecules* **2023**, *28*, 3471. [[CrossRef](#)] [[PubMed](#)]
17. Weightman, P.; Martin, D.S.; Cole, R.J.; Farrell, T. Reflection anisotropy spectroscopy. *Rep. Progr. Phys.* **2005**, *68*, 1251. [[CrossRef](#)]
18. Kamiya, I.; Aspnes, D.E.; Florez, L.T.; Harbison, J.P. Reflectance-difference spectroscopy of (001) GaAs surfaces in ultrahigh vacuum. *Phys. Rev. B* **1992**, *46*, 15894. [[CrossRef](#)] [[PubMed](#)]
19. Hofmann, P.; Rose, K.C.; Fernandez, V.; Bradshaw, A.M.; Richter, W. Study of Surface States on Cu(110) Using Optical Reflectance Anisotropy. *Phys. Rev. Lett.* **1995**, *75*, 2039. [[CrossRef](#)]

20. Goletti, C.; Bussetti, G.; Arciprete, F.; Chiaradia, P.; Chiarotti, G. Infrared surface absorption in Si(111)2×1 observed with reflectance anisotropy spectroscopy. *Phys. Rev. B* **2002**, *66*, 153307. [[CrossRef](#)]
21. Shkrebti, A.I.; Esser, N.; Richter, W.; Schmidt, W.G.; Bechstedt, F.; Fimland, B.O.; Kley, A.; Del Sole, R. Reflectance anisotropy of GaAs (100): Theory and experiment. *Phys. Rev. Lett.* **1998**, *81*, 721. [[CrossRef](#)]
22. Goletti, C.; Bussetti, G.; Violante, A.; Bonanni, B.; Di Giovannantonio, M.; Serrano, G.; Breuer, S.; Gentz, K.K.; Wandelt, K. Cu(110) Surface in Hydrochloric Acid Solution: Potential Dependent Chloride Adsorption and Surface Restructuring. *J. Phys. Chem. C* **2015**, *119*, 1782. [[CrossRef](#)]
23. Yivlialin, R.; Brambilla, L.; Accogli, A.; Gibertini, E.; Tommasini, M.; Goletti, C.; Leone, M.; Duò, L.; Magagnin, L.; Castiglioni, C.; et al. Evidence of graphite blister evolution during the anion de-intercalation process in the cathodic regime. *Appl. Surf. Sci.* **2020**, *504*, 144440. [[CrossRef](#)]
24. Serrano, G.; Bonanni, B.; Kosmala, T.; Di Giovannantonio, M.; Diebold, U.; Wandelt, K.; Goletti, C. In situ scanning tunneling microscopy study of Ca-modified rutile TiO₂(110) in bulk water. *Beilstein J. Nanotechnol.* **2015**, *6*, 438–443. [[CrossRef](#)] [[PubMed](#)]
25. Goletti, C.; Bussetti, G.; Chiaradia, P.; Sassella, A.; Borghesi, A. Highly sensitive optical monitoring of molecular film growth by organic molecular beam deposition. *Appl. Phys. Lett.* **2003**, *83*, 4146. [[CrossRef](#)]
26. Sun, L.; Berkebile, S.; Weidlinger, G.; Koller, G.; Hohage, M.; Netzer, F.P.; Ramsey, M.; Zeppenfeld, P. Revealing the buried interface: Para-sexiphenyl thin films grown on TiO₂(110). *Phys. Chem. Chem. Phys.* **2010**, *12*, 3141. [[CrossRef](#)] [[PubMed](#)]
27. Zhao, B.; Yang, S.; Deng, J.; Pan, K. Chiral Graphene Hybrid Materials: Structures, Properties, and Chiral Applications. *Adv. Sci.* **2021**, *8*, 2003681. [[CrossRef](#)]
28. Nechayev, S.; Barczyk, R.; Mick, U.; Banzer, P. Substrate-Induced Chirality in an Individual Nanostructure. *ACS Photonics* **2019**, *6*, 1876. [[CrossRef](#)]
29. Berg, A.M.; Patrick, D.L. Preparation of Chiral Surfaces from Achiral Molecules by Controlled Symmetry Breaking. *Angew. Chem. Int. Ed.* **2005**, *44*, 1821–1823. [[CrossRef](#)] [[PubMed](#)]
30. Kuroda, R.; Harada, T.; Shindo, Y. A solid-state dedicated circular dichroism spectrophotometer: Development and application. *Rev. Sci. Instrum.* **2001**, *72*, 3802. [[CrossRef](#)]
31. Kuroda, R.; Harada, T.; Takahashi, H. Fast and artifact-free circular dichroism measurement of solid-state structural changes. *Chirality* **2024**, *36*, e3622. [[CrossRef](#)]
32. Kuroda, R. Solid-state Chiroptical spectroscopy-rich information provided but attention needed. Chapter 30. In *Chiral Luminescence: From Molecules to Materials and Devices*; Akagi, K., Ed.; Wiley-VCH. Inc.: Weinheim, Germany, 2023; *in press*.
33. Salvati, A.; Chiaradia, P. Analysis of reflectometers for surface anisotropy. *Appl. Opt.* **2000**, *39*, 5820. [[CrossRef](#)]
34. Kemp, J.C. Piezo-Optical Birefringence Modulators: New Use for a Long-Known Effect. *J. Opt. Soc. Am.* **1969**, *59*, 950–954. [[CrossRef](#)]
35. Berkovits, V.L.; Kiselev, V.A.; Safarov, V.I. Optical spectroscopy of (110) surfaces of III–V semiconductors. *Surf. Sci.* **1989**, *211*, 489. [[CrossRef](#)]
36. Available online: <https://jascoinc.com/products/spectroscopy/circular-dichroism/> (accessed on 10 August 2024).
37. Yang, S.J.; Jung, J.-H.; Lee, E.; Han, E.; Choi, M.-Y.; Jung, D.; Choi, S.; Park, J.-H.; Oh, D.; Noh, S.; et al. Wafer-Scale Programmed Assembly of One-Atom-Thick Crystals. *Nano Lett.* **2022**, *22*, 1518. [[CrossRef](#)] [[PubMed](#)]
38. Kim, C.-J.; Sánchez-Castillo, A.; Ziegler, Z.; Ogawa, Y.; Noguez, C.; Park, J. Chiral atomically thin films. *Nat. Nanotechnol.* **2016**, *11*, 520. [[CrossRef](#)]
39. Goletti, C.; Bussetti, G.; Chiaradia, P.; Sassella, A.; Borghesi, A. In situ optical investigation of oligothiophene layers grown by organic molecular beam epitaxy. *J. Phys. Condens. Matter* **2004**, *16*, S4393. [[CrossRef](#)]
40. Compton, O.C.; Nguyen, S.T. Graphene Oxide, Highly Reduced Graphene Oxide, and Graphene: Versatile Building Blocks for Carbon-Based Materials. *Small* **2010**, *22*, 711. [[CrossRef](#)] [[PubMed](#)]
41. Available online: <https://pnrr.inaf.it/progetto-stiles/> (accessed on 10 August 2024).
42. Hazen, R.M. Geochemical origins of life. In *Fundamentals of Geobiology*; Knoll, A.H., Canfield, D.E., Konhauser, K.O., Eds.; Wiley-Blackwell: Oxford, UK, 2012; pp. 315–332.
43. Hazen, R.M. Enantioselective adsorption on rock-forming minerals: A thought experiment. *Surf. Sci.* **2014**, *629*, 11. [[CrossRef](#)]
44. Available online: <https://hazen.carnegiescience.edu/publications/astrobiology-origin-life> (accessed on 10 August 2024).
45. Song, G.; Hao, H.; Yan, S.; Fang, S.; Xu, W.; Tong, L.; Zhang, J. Observation of Chirality Transfer in Twisted Few-Layer Graphene. *ACS Nano* **2024**, *18*, 17578. [[CrossRef](#)]
46. Carr, S.; Massatt, D.; Fang, S.; Cazeaux, P.; Luskin, M.; Kaxiras, E. Twistronics: Manipulating the electronic properties of two-dimensional layered structures through their twist angle. *Phys. Rev. B* **2017**, *95*, 075420. [[CrossRef](#)]
47. Ciarrocchi, A.; Tagarelli, F.; Avsar, A.; Kis, A. Excitonic devices with van der Waals heterostructures: Valleytronics meets twistronics. *Nat. Rev. Mater.* **2022**, *7*, 449–464. [[CrossRef](#)]
48. Zhu, H.; Yakobson, B.I. Creating chirality in the nearly two dimensions. *Nat. Mater.* **2024**, *23*, 316–322. [[CrossRef](#)]

Disclaimer/Publisher’s Note: The statements, opinions and data contained in all publications are solely those of the individual author(s) and contributor(s) and not of MDPI and/or the editor(s). MDPI and/or the editor(s) disclaim responsibility for any injury to people or property resulting from any ideas, methods, instructions or products referred to in the content.